

ANL/IPNS/CP-86896

RECEIVED

FEB 08 1996

OSTI

CRYSTAL PHASES AND LATTICE DYNAMICS OF SLIP-CAST  
 $\beta'$ -SIALONS

CONF-951155--79

C. K. LOONG\*, J. W. RICHARDSON, JR.\*, S. SUZUKI, \*\* and M. OZAWA\*\*

\*Argonne National Laboratory, Argonne, IL 60439, U. S. A.

\*\*Nagoya Institute of Technology, Tajimi, Gifu, 507, Japan.

The submitted manuscript has been authored by a contractor of the U. S. Government under contract No. W-31-109-ENG-38. Accordingly, the U. S. Government retains a nonexclusive, royalty-free license to publish or reproduce the published form of this contribution, or allow others to do so, for U. S. Government purposes.

Presented at  
The Materials Research Society Fall Meeting  
Boston, MA  
Nov. 27 - Dec. 1, 1995

Proceedings to be published in *Mat. Res. Soc. Symp. Proc.*

\*Work supported by U. S. Department of Energy, BES, contract No. W-31-109-ENG-38

**DISCLAIMER**

This report was prepared as an account of work sponsored by an agency of the United States Government. Neither the United States Government nor any agency thereof, nor any of their employees, makes any warranty, express or implied, or assumes any legal liability or responsibility for the accuracy, completeness, or usefulness of any information, apparatus, product, or process disclosed, or represents that its use would not infringe privately owned rights. Reference herein to any specific commercial product, process, or service by trade name, trademark, manufacturer, or otherwise does not necessarily constitute or imply its endorsement, recommendation, or favoring by the United States Government or any agency thereof. The views and opinions of authors expressed herein do not necessarily state or reflect those of the United States Government or any agency thereof.

MASTER

DISTRIBUTION OF THIS DOCUMENT IS UNLIMITED  
DUC

#### **DISCLAIMER**

**Portions of this document may be illegible  
in electronic image products. Images are  
produced from the best available original  
document.**

# CRYSTAL PHASES AND LATTICE DYNAMICS OF SLIP-CAST $\beta'$ -SIALONS

C.-K. LOONG\*, J. W. RICHARDSON, JR.\*<sup>1</sup>, S. SUZUKI,\*\* and M. OZAWA\*\*

\*Argonne National Laboratory, Argonne, IL 60439, U. S. A.

\*\*Nagoya Institute of Technology, Tajimi, Gifu, 507, Japan.

## ABSTRACT

The crystal structures and phonon densities of states (DOS) of  $\beta'$ -Sialon ceramics,  $\text{Si}_{6-z}\text{Al}_z\text{O}_z\text{N}_{8-z}$  ( $0 \leq z \leq 6$ ), prepared by a novel slip-cast method were studied by neutron scattering techniques. A Rietveld analysis of the diffraction patterns shows that samples of  $z < 4$  form a single-phase solid solution of Si-Al-O-N isostructural to  $\beta\text{-Si}_3\text{N}_4$  (space group  $\text{P}6_3/m$ ). Within this structure there is a consistent preferred occupation of O on the 2c sites and N on the 6h sites. For  $z > 4$  the materials exhibit multiple-phase structure. The observed phonon DOS of the  $0 \leq z \leq 4$  ceramics displays phonon bands at about 50 and 115 meV. These features are considerably broader than the corresponding ones in  $\beta\text{-Si}_3\text{N}_4$  powder. As  $z$  increases, effects due to atomic disorder lead to an overlap of the two phonon bands and a complete fill up of the phonon gap at  $\sim 100$  meV observed in  $\text{Si}_3\text{N}_4$ .

## INTRODUCTION

$\beta'$ -sialon, described by the formula of  $\text{Si}_{6-z}\text{Al}_z\text{O}_z\text{N}_{8-z}$  ( $0 \leq z \leq 4$ ), is formed from a solid solution extended along a constant metal to nonmetal atom ratio (Si,Al):(O,N) within the  $\text{Si}_3\text{N}_4\text{-AlN-Al}_2\text{O}_3\text{-SiO}_2$  system. These ceramic alloys not only retain the outstanding high-temperature properties of silicon nitride (e. g., high strength and hardness, low thermal expansion, and superb chemical durability) but also permit fabrication by conventional green processing such as hot isostatic press method [1-4]. Recently, reaction-sintered  $\beta'$ -sialon ceramics were prepared using aqueous slurries by a slip-casting method [5]. This method provides an inexpensive means to fabricate ceramic components of relatively complex shapes. It is desirable to characterize the crystal phases and atomic dynamics of such slip-cast  $\beta'$ -sialon ceramics in conjunction with the macroscopic properties. This paper reports the results of a neutron-scattering study of the crystal structure and lattice vibrations of  $\text{Si}_{6-z}\text{Al}_z\text{O}_z\text{N}_{8-z}$  ( $0 \leq z \leq 6$ ) materials. Details of the fabrication technique and various mechanical properties have been given elsewhere [5].

## CRYSTAL PHASES

Seven ceramic rods of  $\text{Si}_{6-z}\text{Al}_z\text{O}_z\text{N}_{8-z}$  of nominal compositions  $z = 0, 1, 2, 3, 4, 5$ , and 6 (dimensions  $3 \times 4 \times 40$  mm<sup>3</sup>) were examined by neutron diffraction using the General Purpose Powder Diffractometer (GPPD) at the Intense Pulsed Neutron Source (IPNS) of Argonne National Laboratory. A resolution of  $\Delta d/d = 0.25\%$  (where  $d$  is the atomic spacing) can be achieved from the back-scattering geometry. The crystal structure of  $z = 0$  to 4 samples, analyzed by the Rietveld method, was found to be identical to that of  $\beta\text{-Si}_3\text{N}_4$  (hexagonal,  $\text{P}6_3/m$ ). They can be described by the formula  $\text{Si}_{6-z}\text{Al}_z(\text{O}_y\text{N}_{6-y})(\text{O}_x\text{N}_{2-x})$  with  $x + y = z$  and  $0 \leq z \leq 4$  of which the Si or Al occupy the 6h ( $u, v, 1/4$ ) sites, O(1) or N(1) atoms within the first parentheses occupy the 6h site and O(2) or N(2) within the second parentheses occupy the 2c ( $1/3, 2/3, 1/4$ ) sites. A typical observed and fitted powder pattern is given in Fig. 1.

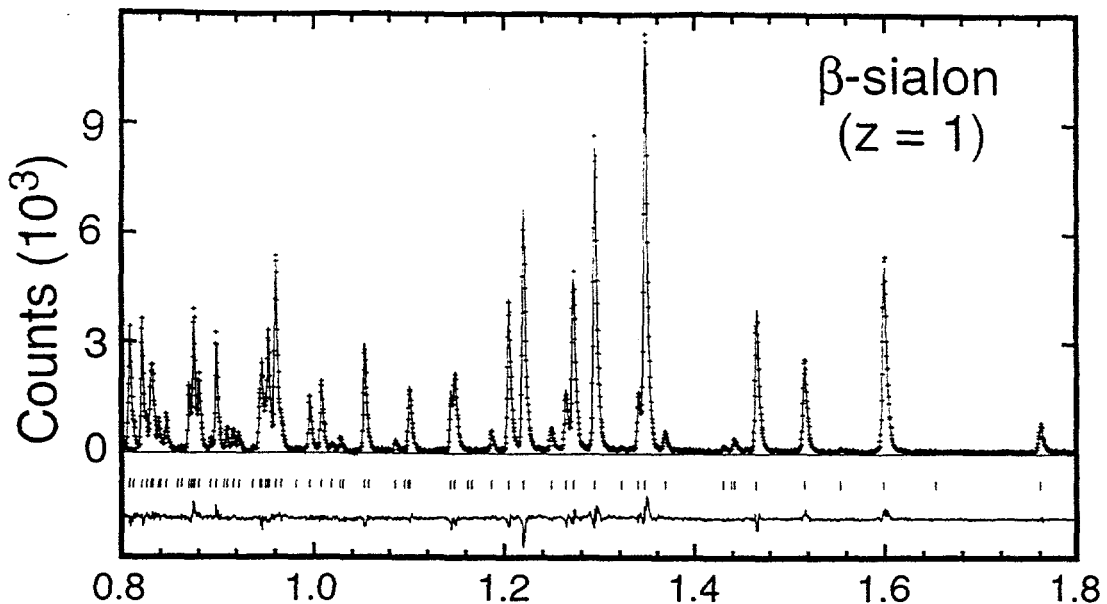


Figure 1. Rietveld profile fit in the 0.8-1.8  $\text{\AA}$  region of d-spacing for the  $z = 1$  sialon sample. The symbols are the observed, background subtracted intensities. The solid line represents the calculated crystalline intensities. The tick marks indicate the positions of the Bragg reflections. The difference between the observed and calculated intensities are shown at the bottom of the figure.

The major findings concerning the crystal structure of the  $z = 0$ -4 samples are summarized as follows:

1. The compositions are  $\text{Si}_6\text{N}_8$ ,  $\text{Si}_5\text{AlO}_{0.990}\text{N}_{7.010}$ ,  $\text{Si}_4\text{Al}_2\text{O}_{1.848}\text{N}_{6.152}$ ,  $\text{Si}_3\text{Al}_2\text{O}_{3.102}\text{N}_{4.898}$ , and  $\text{Si}_2\text{Al}_4\text{O}_{3.812}\text{N}_{4.188}$  for  $z = 0$  to 4, respectively. In the structural refinement, the normal  $z$  values and random substitution of Si by Al were assumed because the data were not sufficient to resolve the distributions of Si and Al atoms over the 6h sites. The weighted R-values are less than 8%.
2. The entire crystalline phase of the  $z = 0$ -3 samples can be accounted for by the  $\beta$ - $\text{Si}_3\text{N}_4$ -type structure. For the  $z = 4$  sample a few weak impurity peaks were observed.
3. The amount of vacancy-related defects in the crystalline phase of the materials, if any, is very small.
4. The structural refinements show evidence of preferred occupation of O(2) on the 2c sites and N(1) on the 6h sites, in good agreement with previous neutron diffraction results of  $\beta'$ -sialon powders prepared by different methods [6-7].
5. The lattice expands as increasing number of Si and N atoms are replaced by Al and O, respectively. At  $z = 1$  the nearest neighbor distances between the metal atoms (Si, Al) and the nonmetal atoms (N, O) coincide, which indicates a relatively uniform interatomic distances in the  $\text{M}_3(\text{N},\text{O})$  triangles oriented parallel and normal to the basal plane. For larger  $z$ , significant distortion of the framework triangles results from a disparity of the M-(N,O) distances.
6. The average crystalline grain size increases from  $\sim 0.3 \mu\text{m}$  for  $z = 1$  to  $> 0.6 \mu\text{m}$  for  $z = 4$ . Scanning electron microscopy measurements show that the  $z = 1$  sample has the finest, elongated grains, and the grain size grows considerably with decreasing aspect ratio as  $z$  increases. These results are consistent with the optimal mechanical performance of the slip-cast  $\beta'$ -sialons near  $z = 1$  [5].

Details regarding correlation between the crystal structure and the macroscopic properties of the  $z = 0$ -4 materials have been presented elsewhere [8].

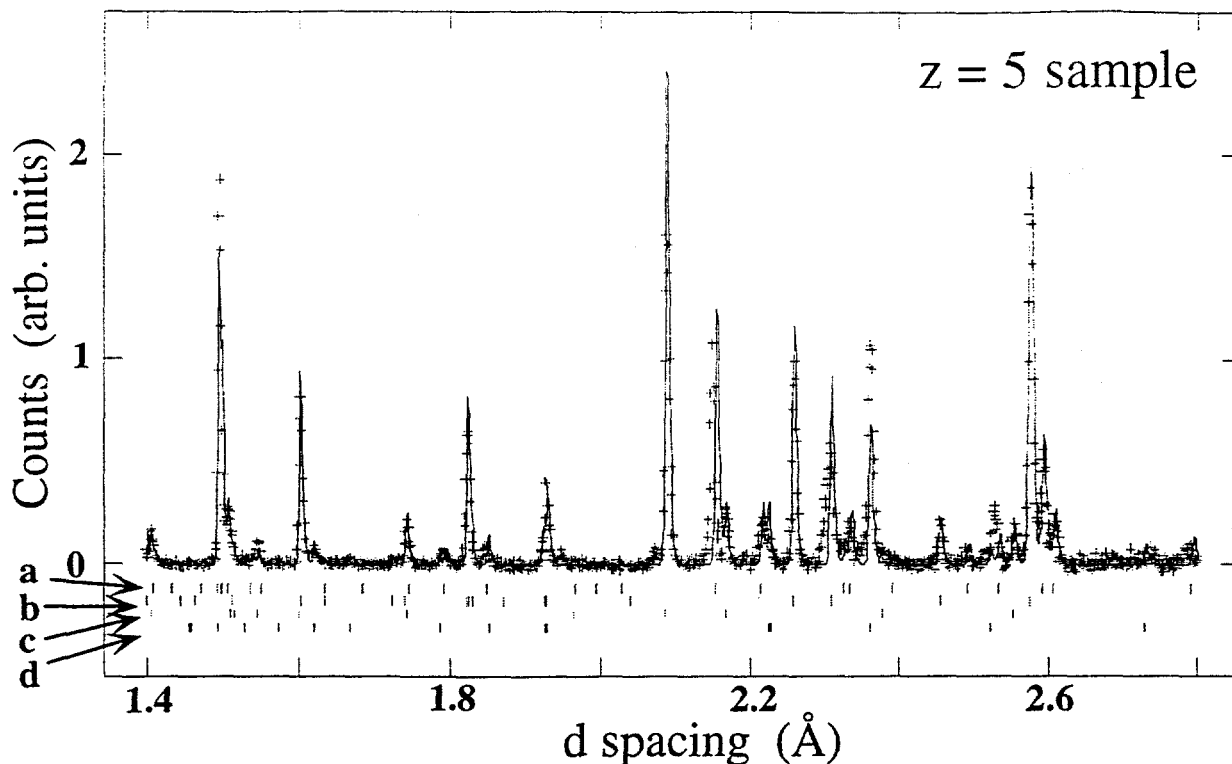


Figure 2. Rietveld profile fit in the 1.4-2.8 Å region of d-spacing for the  $z = 5$  sample. The crystalline phases labeled a, b, c, and d correspond to  $\text{SiAl}_5\text{O}_5\text{N}_3$ ,  $\theta\text{-Si}_3\text{Al}_{12}\text{O}_9\text{N}_{10}$ ,  $\alpha\text{-Al}_2\text{O}_3$ , and  $\beta'\text{-SiAl}_4\text{O}_2\text{N}_4$ , respectively. The LeBail technique was applied to the fit whereby structure factor calculations for the  $\theta\text{-Si}_3\text{Al}_{12}\text{O}_9\text{N}_{10}$  and  $\beta'\text{-SiAl}_4\text{O}_2\text{N}_4$  phases were ignored.

$\beta'$ -sialon as  $\text{Si}_{6-z}\text{Al}_z\text{O}_z\text{N}_{8-z}$  does not form single-phase materials for  $z > 4$ . Instead, complex multiple crystalline phases are observed. A portion of the powder pattern of the  $z = 5$  ceramic is shown in Fig. 2 where only a minute (~6%)  $\text{SiAl}_5\text{O}_5\text{N}_3$  having the  $\beta'$ -sialon crystal structure remains. The predominant phase in the  $z = 5$  sample is  $\alpha\text{-Al}_2\text{O}_3$ . The ratio of  $\alpha\text{-Al}_2\text{O}_3$  to  $\text{SiAl}_5\text{O}_5\text{N}_3$  was estimated from the Rietveld analysis to be about 1:92. Two other phases, identified according to the JCPDS powder diffraction files as monoclinic  $\theta\text{-Si}_3\text{Al}_{12}\text{O}_9\text{N}_{10}$  and rhombohedral  $\beta'\text{-SiAl}_4\text{O}_2\text{N}_4$ , but not refined structurally, are also shown in Fig. 2.

The predominant phase in the  $z = 6$  sample was identified as the cubic phase  $\text{Al}_3\text{O}_3\text{N}$  having the same structure as  $\text{Al}_2\text{MgO}_4$ . A refinement using this structure, as shown in Fig. 3, resulted in a composition of  $\text{Al}_3\text{O}_{2.9}\text{N}_{1.1}$ . Many of the additional reflections can be indexed with a monoclinic cell,  $a = 20.1$ ,  $b = 2.7$ ,  $c = 10.8$  Å, and  $\beta = 119^\circ$ , but the composition is not known at the present time.

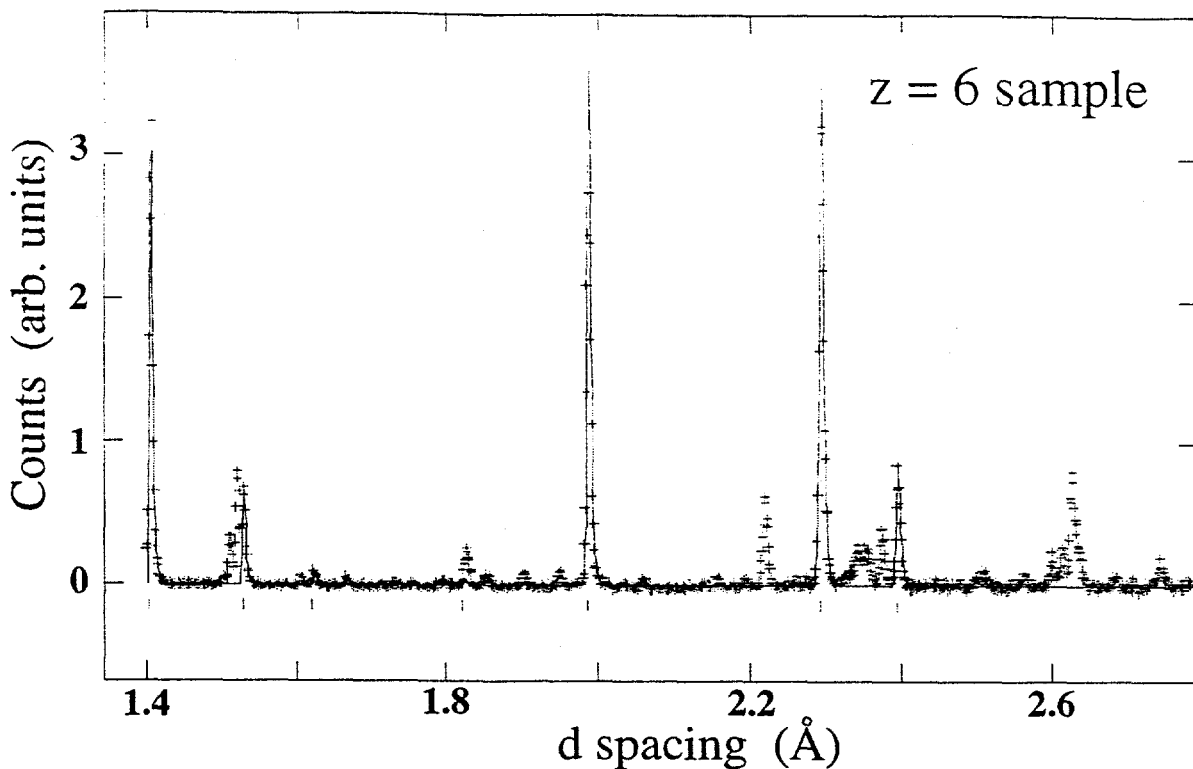


Figure 3. Rietveld profile fit in the 1.4-2.8 Å region of d-spacing for the  $z = 6$  sample. Only the  $\text{Al}_3\text{O}_3\text{N}$  phase was used in the fit.

## PHONON DENSITIES OF STATES

The generalized (neutron cross-section weighted) phonon densities of states (DOS) of the  $z = 0$ -4 slip-cast  $\beta'$ -sialon ceramics (dimension  $30 \times 70 \times 5 \text{ mm}^3$ ) were determined by neutron inelastic-scattering using the High-Resolution Medium-Energy Chopper Spectrometer (HRMECS) of IPNS. An incident energy ( $E_0$ ) of 200 meV was used for the measurements. The energy resolution  $\Delta E$  (full width at half-maximum) of HRMECS varies from  $\sim 4\%$  of  $E_0$  in the elastic region to  $\sim 2\%$  near the end of the neutron energy-loss spectrum. Fig. 4 displays the measured DOS of the  $\beta'$ -sialon ceramics and a comparison with that of a pure  $\beta$ - $\text{Si}_3\text{N}_4$  powder. The spectra, which were normalized to give the same integrated area, show a one-phonon DOS extending to  $\sim 170$  meV ( $1371 \text{ cm}^{-1}$ , 1 meV is equivalent to  $8.066 \text{ cm}^{-1}$ ) with two broad bands centered at about 50 and 115 meV. The low-energy region ( $< 40$  meV) involves mainly the lattice vibrations of the tetrahedra network. The 50-meV and 115-meV bands may be assigned to bending and stretching of the  $\text{Si}(\text{Al})\text{-N}(\text{O})$  bonds, respectively. The DOS of the  $z = 0$  ceramic resembles closely that of the  $\text{Si}_3\text{N}_4$  powder excepting the somewhat sharper features in the powder sample [9]. This probably reflects a larger strain distribution over the crystalline grains in the ceramic sample resulted from the sintering process. As Si and N are replaced by Al and O in the  $z \geq 1$  samples, the two vibrational bands broaden and the phonon densities in the 60-90 meV and 130-150 meV regions increase progressively. A slight increase of density below  $\sim 30$  meV as increasing  $z$  can also be seen. Thus the atomic dynamics shows a distinct response to the bonding environment due to chemical disorder over a wide range of vibrational frequencies.

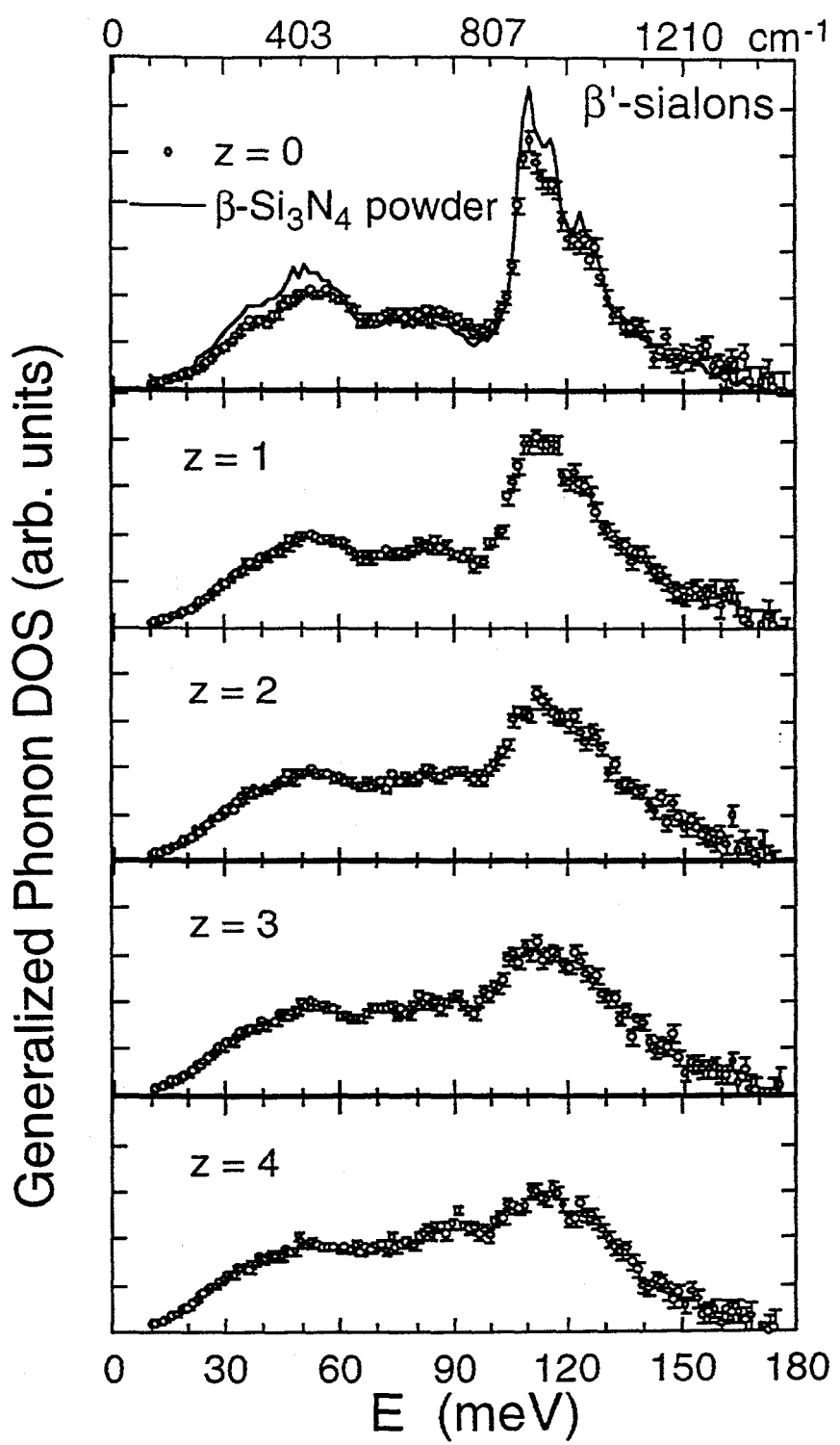


Figure 4. The measured generalized phonon densities of states of  $\beta'$ -sialon ceramics and  $\beta$ - $\text{Si}_3\text{N}_4$  powder.

Lattice dynamics calculations of  $\text{Si}_3\text{N}_4$  have been reported by Wendel and Goddard [10] and by Mirgorodsky and coworkers [11]. A gap centered at about 90 meV in the phonon spectrum of  $\beta\text{-Si}_3\text{N}_4$  was found. Qualitatively, the gap divides the low-frequency out-of-plane motion of atoms in the coplanar  $\text{N}(2)\text{Si}_3$  and the nearly coplanar  $\text{N}(1)\text{Si}_3$  units from the high-frequency in-plane Si-N stretch vibrations. The phonon gap, smeared by the instrumental resolution, is seen in Fig. 4 as a dip at about 95 meV in the measured DOS of  $\beta\text{-Si}_3\text{N}_4$ . In  $\beta'$ -sialon ceramics these two portions of the DOS are broaden and the phonon gap is filled progressively as  $z$  increases. Therefore, the neutron results indicate that chemical disorder severely affect the density distribution of the high-energy Si(Al)-N(O) stretch and the low-energy Si(Al)-N(O) out-of-plane bending modes. The increase of ionicity in the bonding also reduce the disparity between force constants corresponding to the in-plane and out-of-plane atomic vibrations in the  $\text{NSi}_3$  units.

We thank Mr. T. Nasu for his help in sample preparation and Mr. J. Nipko and Dr. S. Skanthakuma for their assistance in the collection and refinements of the powder-diffraction data. We are also grateful to Dr. P. Vashishta for many helpful discussions. Work performed at Argonne National Laboratory is supported by the U. S. DOE-BES under Contract No. W-31-109-ENG-38.

## REFERENCES

- 1 K. H. Jack, in *Silicon nitride ceramics: scientific and technological advances* (eds. I.-W. Chen, P. F. Becher, M. Mitomo, G. Petzow and T.-S. Yen) p. 15 (Materials Research Society, Pittsburgh, PA, 1993).
- 2 T. Ekström, in *The encyclopedia of advanced materials* (eds. D. Bloor, M. C. Flemings, R. J. Brook and S. Mahajan) p. 2444 (Pergamon, Oxford, 1994).
- 3 T. Ekström and M. Nygren, *J. Am. Ceram. Soc.*, **75** 259 (1992).
- 4 M. H. Lewis, in *Silicon nitride ceramics: scientific and technological advances* (eds. I.-W. Chen, P. F. Becher, M. Mitomo, G. Petzow and T.-S. Yen) p. 159 (Materials Research Society, Pittsburgh, PA, 1993).
- 5 S. Suzuki, T. Nasu, S. Hayama, and M. Ozawa, *J. Am. Ceram. Soc.* (Submitted).
- 6 L. Gillott, N. Cowlam, and G. E. Bacon, *J. Mat. Sci.*, **16** 2263 (1981).
- 7 F. K. van Dijen, R. Metselaar, and R. B. Helmholdt, *J. Mat. Sci. Lett.*, **6** 1101 (1987).
- 8 C.-K. Loong, J. W. Richardson, Jr., M. Ozawa, and S. Suzuki, *J. Am. Ceram. Soc.* (submitted).
- 9 C.-K. Loong, P. Vashishta, R. K. Kalia, and I. Ebbsjö, *Europhys. Lett.*, **31** (4), 201 (1995).
- 10 J. A. Wendel and W. A. Goddard III, *J. Chem. Phys.*, **97** (7), 5048 (1992).
- 11 A. P. Mirgorodsky, M. I. Baraton, and P. Quintard, *Phys. Rev.*, **B 48** (18), 13326 (1993).